Experimental investigation of cavitating flow in 2D and 3D transparent diesel nozzle models

Cyril Mauger, Loïc Méès, Marc Michard, Stéphane Valette

Experimental investigation of cavitating flow in 2D and 3D transparent diesel nozzle models

C. Mauger[1], L. Méès[1], M. Michard[1], S. Valette[2]

1: Laboratoire de Mécanique des Fluides et d'Acoustique, UMR CNRS 5509,
Ecole Centrale de Lyon, INSA de Lyon and Université Claude Bernard,
36 avenue Guy de Collongue, 69134 Ecully France

2: Laboratoire de Triboligie et Dynamique des Système, UMR CNRS 5513,
Ecole Centrale de Lyon, Ecole Nationale des Mines de Saint Etienne,
Ecole Nationale d'Ingénieurs de Saint Etienne
36 avenue Guy de Collongue, 69134 Ecully France

Corresponding Authors : loic.mees@ec-lyon.fr, cyril.mauger@ec-lyon.fr

Abstract: The paper describes two experimental set-up dedicated to the study of cavitation in diesel injectors. The two experimental set-up are described and preliminary results are presented. The first approach consists of flow characterization in 3D and real-size transparent injector. A second approach deals with a 2D injector and is dedicated to the specific study of surface roughness effect on cavitation processes.

Keywords: Cavitation, transparent nozzle, experimental visualization, roughness surface, CFD

1. Introduction

Diesel engine efficiency and air pollution emissions are strongly dependent on the fuel atomization happening in the combustion chamber. Fuel atomization is obtained by discharging highly pressurized fuel through very small orifices. The injection pressure is provided by a common rail system and can reach 200 MPa. Orifices are typically about 100 μm and flow velocities reach several hundred meters per second. Under such conditions, the flow can be locally turbulent and sometimes cavitating [1].

Cavitation reduces the discharge coefficient and therefore the mass flow rate. The number of orifices is increased to compensate for the drop in mass flow rate. Cavitation can induce vibrations and noise pollution [2]. Yet, cavitation may also prevent nozzle fouling and enhance atomization [2-5]. Understanding how turbulence and cavitation impact atomization is essential to open up new prospects of development.

In injectors, there is a strong change in the cross-section between the sac volume and the orifice entrance. This forces the flow to change its direction. At the inlet of the injection hole, the curvature of the streamlines tends to separate the boundary layer from the wall. Some recirculation zones are formed at the inlet and a so-called *vena contracta* occurs. The flow reattaches to the wall located behind the recirculation zones. The resulting inlet contraction significantly reduces the area available for the liquid flow. The reduced area is accompanied by increased velocity, as a consequence of mass conservation. So, the acceleration of the liquid throughout the *vena contracta* entails a depression in the nozzle throat.

In addition to the *vena contracta* effect, flow is strongly shears in the recirculation zones due to a large velocity gradient at the hole inlet. The presence of high shear viscous stress further restrains the flow. Joseph [6] suggested that total stress, which includes both pressure and viscous stress, plays an important role in cavitation. In other words, cavitation occurs when the maximum principal stress drops below the breaking strength of the liquid. Yet, in numerical approaches few cavitation models are based on the total-stress criterion to predict cavitation inception [7, 8].

The combination of the recirculation zones with the strong shear may cause cavitation at the inlet of the hole [11]. Cavitation appearance is strongly favored by cavitation germs included in the liquid as gaseous inclusions, and by geometrical irregularities, including surface roughness.

Carried away by the flow, cavitation develops along the orifice wall and eventually disintegrates into bubble clusters which in turn collapse further in the hole, where the pressure increase again. The bubble implosion creates flow disturbance. When the flow velocity is high enough, it may carry away bubbles at the nozzle exit. Then, bubbles collapse and may give birth to ligaments in the liquid jet [9].

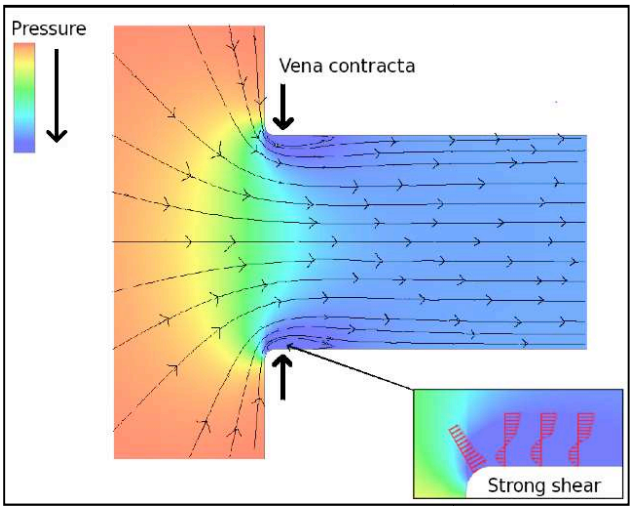

Figure 1: Representation of the pressure field and streamline in a diesel injector orifice inlet

CFD codes are not yet efficient to predict precisely how cavitation occurs and how bubbles collapse in injectors. To gain in efficiency, codes need experimental data that both highlight the parameters possibly promoting cavitation in injectors and quantify the impact of these parameters.

Several studies have already highlighted that inlet radius [3, 10, 11], hole taper [11, 12], fluid properties [13] and walls roughness [11, 14] influence cavitation inception. However, these data are not yet sufficient to devise cavitation models that would make it possible to design tomorrow's injectors.

This paper deals with two test rigs designed using simplified nozzle geometries in order to facilitate flow measurements and comparisons with numerical results.

The first set-up, which is derived from the work of Saliba [15], aims to study how cavitation occurs in a real-size transparent nozzle. Geometric parameters (e.g. inlet hole radius, hole taper, etc.) are investigated at cavitation inception. The internal flow in the sac volume and the orifice is characterized by shadowgraphy. An original lighting method is used.

The second experimental set-up is designed to explore how surface roughness affects the generation of cavitation in a 2D-nozzle. The commercial CFD code named Ansys Fluent was used to predict how cavitation would occur in the 2D-nozzle.

2. Real-size transparent nozzle

It is important to study cavitation in real-size nozzles because cavitation in scaled-up injectors does not occur exactly in the same way [16]. In other words, cavitation phenomena in nozzles cannot be scaled. Chaves [17] explains that cavitation has its own length scale determined by the characteristic collapse time of a given cavity and the flow velocity carrying the cavity. In small nozzles, the typical transit time of a fluid element crossing the orifice is comparable to the time required for a cavity to collapse. Even if scaled-up injector studies have brought interesting information, real-size injector studies are necessary to understand how cavitation occurs and develops in industrial situation of interest.

2.1 Test rig and transparent nozzle

An experimental setup has been developed to visualize the two-phase flow in a real-size transparent nozzle. A high-pressure pump supplies ISO 4113 oil to a common rail which is connected to a standard solenoid injector. The fluid pressure is monitored through a sensor fixed through the common rail and the injector. The pump is driven by an electronic unit to fine control the common rail pressure. The injector is also equipped with a needle lift sensor. A computer unit equipped with a data acquisition board monitors injection parameters and visualization triggers as well as data acquisition.

The nozzle of a car engine injector is machined above the original holes (Figure 2). The nozzle end is then replaced by a transparent single hole, machined in a PMMA (polymethyl methacrylate) disk. The transparent nozzle is glued to an intermediate metallic part. The PMMA refractive index is close to that of oil although some index mismatching is clearly seen in the next sections.

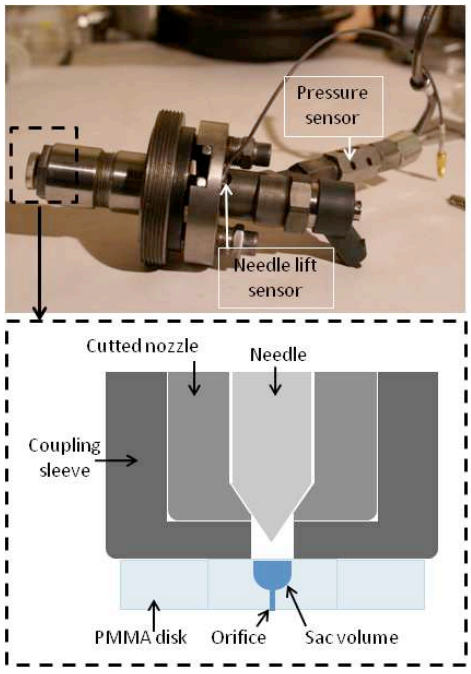

Figure 2: Details of the tip of the injector

This assembly has a limited use. After a certain number of injections, the PMMA disc may unstick or break, depending on the injection pressure.

2.2 Imagery device

Flow visualizations in a real-size injector orifice for real injection conditions are difficult. Very high velocities (typically several hundred meters per second) occur in the orifice. The lighting time must be sufficiently short to avoid image blurring, typically a few nanoseconds, depending on flow velocity and image magnification. The injector is placed in a chamber and a long distance microscope is used to obtain high magnification and resolution (the field of interest is very small, about 1mm*1mm). Due to the small aperture angle of such an optical device, a powerful illumination is required for the resulting intensity to be high enough. An image intensifier may be used but it increases dramatically image noise.

An original lighting method has been used to visualize the flow inside the transparent nozzle. It consists in producing white-light continuum by means of a short (5 ns) and intensive (50 mJ) laser pulse that focuses in ambient air. To do so, a pulsed Nd:YAG laser (λ= 532 nm) with a collimating lens set (Figure 3) is used. Continuum is emitted for 10 to 20 ns. The internal flow is visualized by using a long distance microscope. The field of visualization approximately covers a 1,300x1,000 μm^2 area, which corresponds to a spatial resolution of 1 μm per pixel. Images are recorded on a 12 bits digital CCD camera.

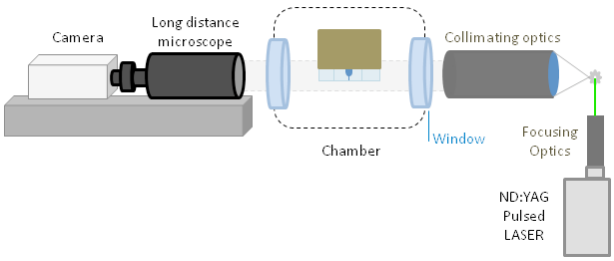

Figure 3: Experimental set-up for flow visualization

Figure 5 is an example of a shadowgraph image, showing the bottom of the sac volume in the upper part, the nozzle orifice and the beginning of the spray in the lower part. The index matching between PMMA and ISO 4113 is not perfect leading to a shadowing of the orifice edges, as clearly visible in Figure 5, where no cavitation occurs. This difference is emphasized by the small surface curvature of the orifice.. Apart from the orifice edge, light areas correspond to liquid phases whereas dark areas correspond to vapor phases.

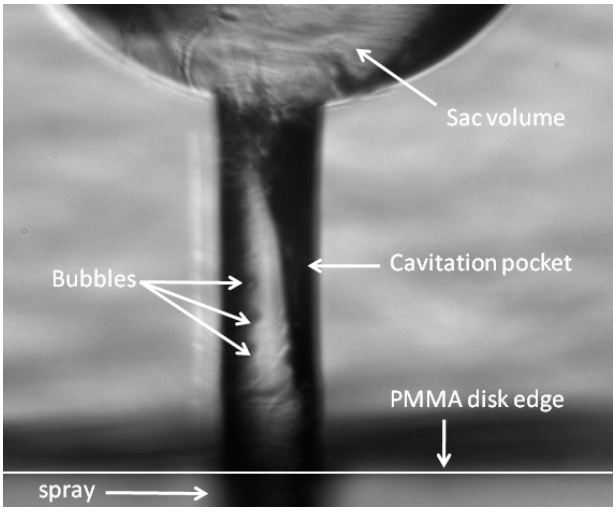

Figure 4: Cavitating flow in a 200 μm diameter orifice

Note that the spray in Figure 4, image is out of focus. Image cannot focus simultaneously on both spray and internal flow, due to the optical distance difference, though and out of PMMA. As an example, Figure 5 shows an image focusing on the spray. The internal flow is now out of focus.

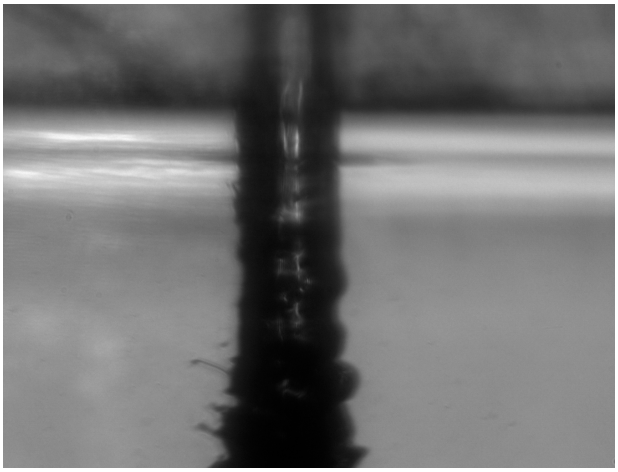

Figure 5: Image of the spray, 390 μs after injection trigger with 250 bar injection pressure

2.3 Results

The geometrical characteristics of the orifice have been optically estimated. Figure 6 shows sac volume and orifice filled with oil, without flow. Orifice diameter and length are 200 μm and 1,000 μm, respectively. The orifice inlet and outlet are slightly convergent and divergent. Radius curvature inlet is estimated to be about 20 μm. A 35 μm eccentricity is noted between the orifice centerline and the sac volume centerline. This offset is located in the image plane (no offset in perpendicular views). It leads to an asymmetric behavior of cavitation which facilitates its visualization.

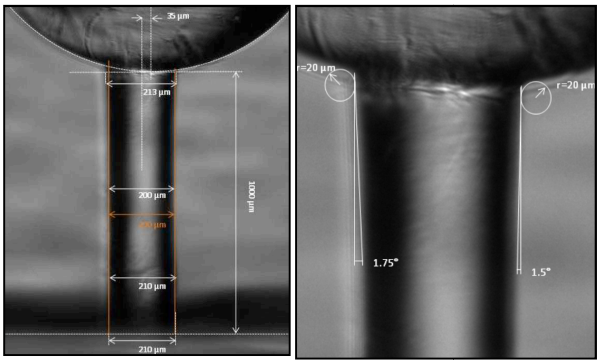

Figure 6: Dimensions of the real-size orifice

The channel shows surface defaults due to machining. It may be interesting to determine whether these defaults (irregularities) influence cavitation formation.

Images are recorded for 25 MPa injection pressure and at different delays between the injection trigger and image acquisition. For each delay, 50 images were recorded over different injection cycles. Needle lift curves corresponding to a single time delay (400 μs) are displayed in Figure 7 (in blue). The same graph displays the average needle lift curve (in red), the injection command signal (in green) and the laser output (in black). This figure clearly shows some needle lift variation from cycle to cycle (note that these variations decrease for increasing injection pressures). As a consequence, images recorded at the same time delay also present significant differences. Then, averaged images have been considered for each time delay and some of them are given in Figure 8.

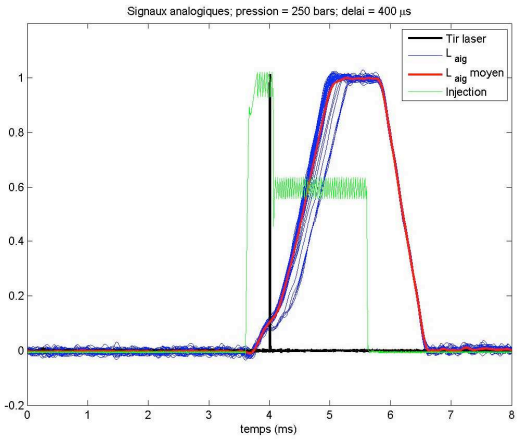

Figure 7: Analog signals recorded aver 50 cycles for 25 MPa injection pressure and 400 μs time delay between injection command and image recording.

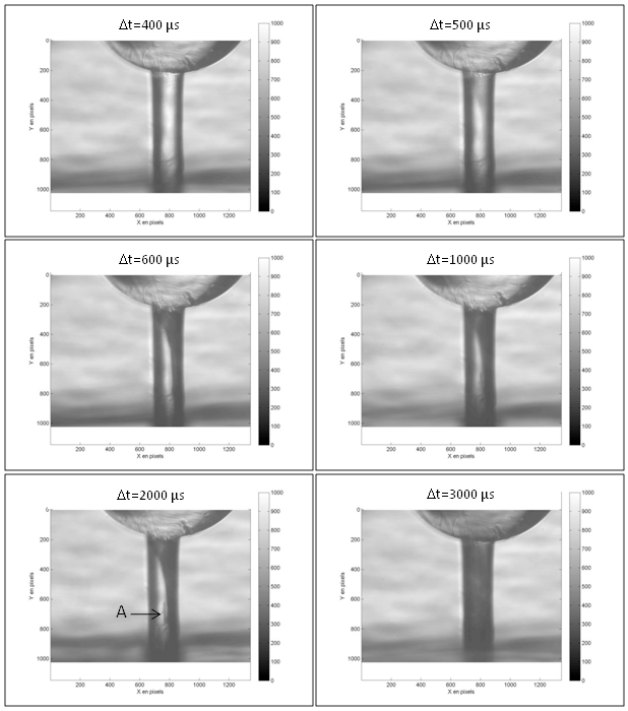

Figure 8: Averaged images for various time delays between injection command and image recording. Injection pressure equals 250 bar

At Δt =400 μs, the oil is flowing inside the channel (a spray is visible at the bottom of the image) but the flow is not yet cavitating. Cavitation appears between 500 and 600 μs, that is to say, for a needle lift of about 10% of its maximum value, at the change of slope in the curves of Figure 7. The cavitation region is asymmetric as a consequence of the orifice eccentricity. For greater time delay, during the needle lift and when the needle has reached the plateau (1000 and 2000 μs), the repartition of vapor in the orifice remains nearly unchanged. When the needle decreases at the end of tinjection (3000 μs) the whole orifice is filled with vapor. In summarize, cavitation appears very soon at the beginning of the injection cycle and quickly stabilizes. To introduce the next section, let us note a detail marked “A” in figure 8. The black vertical line corresponds to a cavitation region which is not connected with the main cavitation pocket. This short line appears and develops from 800 μs time delay. It is probably due to a geometric singularity at the wall orifice, too small to be detected on images without cavitation. Such surface irregularities may emphasis cavitation development and justify specific study of wall roughness effect on cavitating flow.

3. 2D-nozzle

In order to study how roughness may affect a cavitating flow in injector’s orifices, a 2D-nozzle experiment has been designed.

Badock *et al.* [14] stated that cavitation behavior is not well represented in a 2D-nozzle due to nozzle geometry and needle influences. In other words, in a 2D-nozzle cavitation does not behave in the same way as in a 3D-nozzle. Yet, it is much easier to optically observe cavitation forming in a 2D-nozzle; this helps get information that cannot be gained with a 3D-nozzle.

3.1 Test rig and 2D-nozzle

A schematic diagram of the experimental apparatus used in this study is shown in Figure 9. A high-pressure pump ① delivers test oil (ISO 4113) to the 2D-nozzle ⑩ described below. The ISO 4113 oil properties are close to diesel's; they are summarized in Table 1. The oil flow entering the nozzle and upstream pressure are controlled by a by-pass ⑤ while a metering valve ⑪ monitors downstream pressure. A variable area meter ⑥ measures the flow rate. Oil pressure levels are measured 40 mm upstream and downstream of the 2D-nozzle using metal thin film sensors ⑧ and ⑨. Oil temperature in the supply duct of the nozzle is controlled by a T-type thermocouple ⑦. Before returning to the oil tank, the flow goes through an air cooler ⑫ to limit the increase in oil temperature. The hydraulic helps study cavitation forming in continuous state.

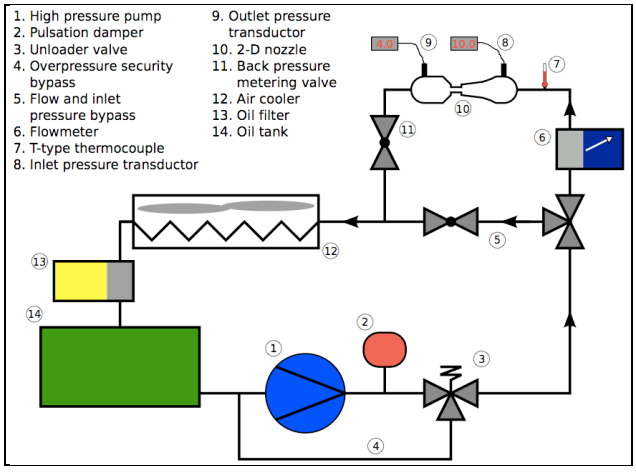

Figure 9: Experimental hydraulic circuit

A 2-D nozzle has been designed for this study (Figure 9a). It is derived from the one used by Winklhofer *et al.* [11]. ISO 4113 oil flows through a rectangular hole (Figure 9b) made of a two-part steel sheet sandwiched between two glass windows. At the upstream of the 2D-nozzle, the flow is calmed by a convergent with a constant acceleration to limit fluctuations before the nozzle inlet. Then, a steep change in cross-section is observed and the flow is forced through a restricted area (Figure 10b). This causes a major pressure drop with high flow stress and cavitation may occur. At the outlet of the 2D-nozzle, the flow is discharged in a liquid volume.

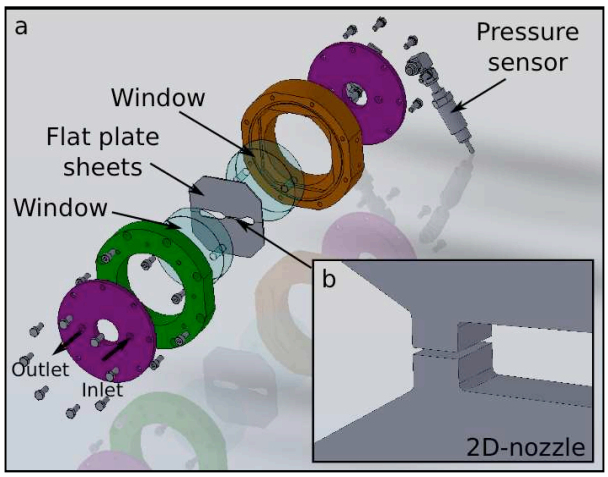

Figure 10: Experimental 2D-nozzle set-up

3.2 Geometry and roughness characterization

To study the influence of the geometry and the roughness on the flow, it is necessary to precisely know the surface conditions and dimensions of the nozzle. A scanning electronic microscope (SEM) is used to assess the 2D-nozzle geometry (Figure 11). In this way, it is possible to measure the nozzle inlet length, height and radius.

A 2 mm thick 2D-nozzle is used in this study. Nozzle height and length are 210 μm and 1,430 μm, respectively. The length / hydraulic diameter ratio is above 3.8 and inlet radius is 11.5 μm. Orifice shape is convergent-divergent.

The SEM helps visualize surface roughness aspect but does not measure it.

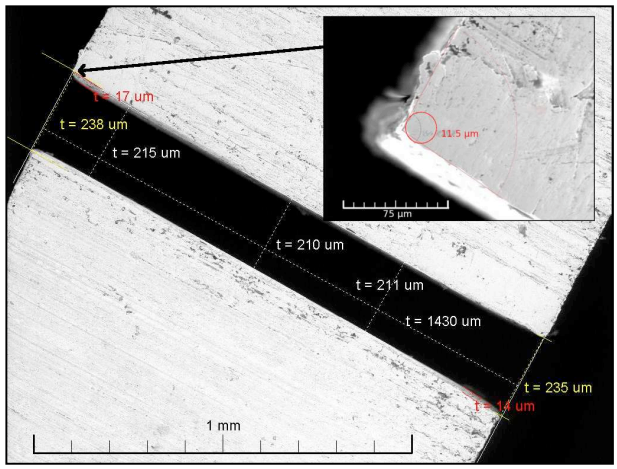

Figure 11: Example of SEM visualization of 2D-nozzle

The separable two-part steel sheet makes it possible to examine orifice walls easily. To know precisely the surface roughness characteristics, a 3D-

interferometer is used. This kind of device helps investigate the roughness properties of a surface. Figure 12 shows an example of 3D-interferometer data acquisition.

	ISO 4113 oil	Diesel
Liquid phase:		
Density ($kg.m^{-3}$)	[ab]828	[c]830
Dynamic viscosity ($kg.m^{-1}.s^{-1}$)	[ab]2.84 10^{-3}	[c]3.32 10^{-3}
Surface tension ($N.m^{-1}$)	-	[c]0.019
Saturation pressure at 40 °C (Pa)	[b]5240	<1000
Vapor phase:		
Density ($kg.m^{-3}$)	7	9.4
Dynamic viscosity ($kg.m^{-1}.s^{-1}$)	1 10^{-5}	7 10^{-6}

[a] at 25 °C, 10 Mpa [b] Rodriguez-Anton relations (2000) [c] Fluent Ansys v12 data base

`Table 1 : ISO 4113 oil and diesel properties

One of the roughness characteristics often employed to determine surface conditions is the arithmetical mean roughness named R_a. It is defined as an integral of the absolute value of the roughness profile measured over an evaluation length.

Interferometry investigation indicates that R_a is 0.45 μm and 0.43 μm for the wall orifice.

3.3 Prediction of flow behavior in a 2D-nozzle using commercial CFD calculation

The commercial CFD software Ansys Fluent v12 is used to perform the numerical simulation of the flow inside the 2D-nozzle Thanks to SEM visualization, the exact geometry of the 2D-nozzle is reproduced and used in a 3D CFD simulation. For this study, surface finishing is considered as perfectly smooth. The computational domain and its mesh are presented in Figure 13. A tetrahedral mesh type was chosen because of the complexity of the 2D-nozzle geometry. The mesh quality of the orifice area is refined.

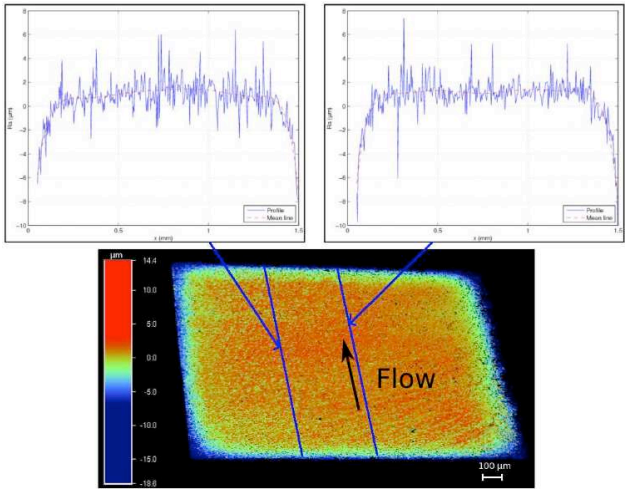

Figure 12: Example of 3D-interferometer data of an orifice wall with surface profiles

A study on the influence of mesh density was carried out and mass flow rates were compared for each mesh. Finally, a mesh of approximately 308,000 nodes is found to be satisfactory to simulate the flow. In calculations, the standard k-ε model was used with a pressure-based coupled algorithm.

Ansys Fluent v12 proposes three different cavitation models. The Schnerr and Sauer [18] model was chosen with the mixture multiphase model. A no-slip condition between the liquid and the vapor phase is assumed. The Schnerr and Sauer model is based on the generalized Rayleigh-Plesset equation, describing the growth of a single spherical vapor bubble in a liquid. In this model, only the number of spherical bubbles per volume of liquid and the fluid vapor saturation pressure must be determined.

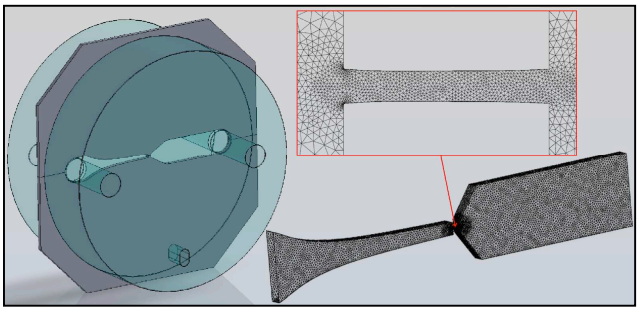

Figure 13: Mesh of the computational domain with detailed mesh of the orifice area

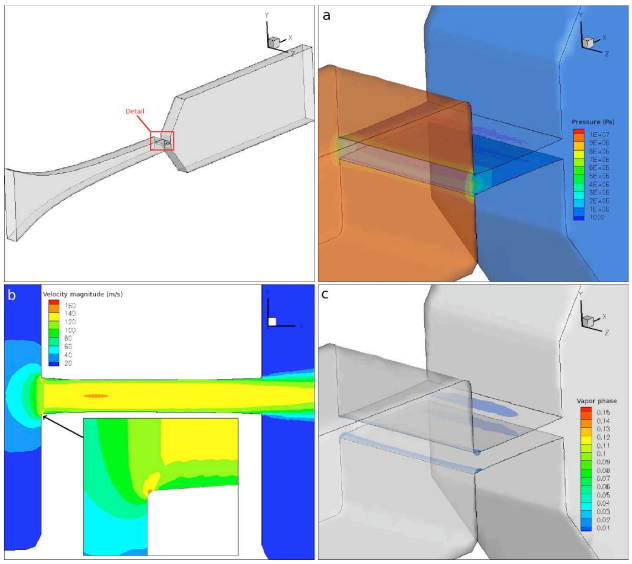

Figure 14: Examples of CFD result for 10 MPa pressure injection and 0.8 MPa back-pressure. a: Pressure field contours. b: Slice of velocity magnitude field. c: Vapor phase field.

The fluid properties used for computation are those of diesel. A gas inclusion number density of about 10^{12} bubbles.m^{-3} was set [19, 20]. Converged calculations were considered when the residuals of

all equations had reached a value of at least 10^{-5} or 10^{-4} at low back-pressure. All calculations are performed in accordance with the experimental set-up underway, i.e. at an injection pressure of 10 MPa. The back-pressure varied from 9 MPa to 0.08 MPa. Examples of pressure, velocity magnitude and cavitation fields in a 2D-nozzle are shown in Figure 14.

Low-pressure areas occur at the inlet corner and convergent zone of the 2D-nozzle (dark-blue areas in Figure 14a). Vapor phase is predominantly produced in these areas (Figure 14c). The velocity magnitude field shows high-speed areas in the near the orifice centerline and in inlet corner.

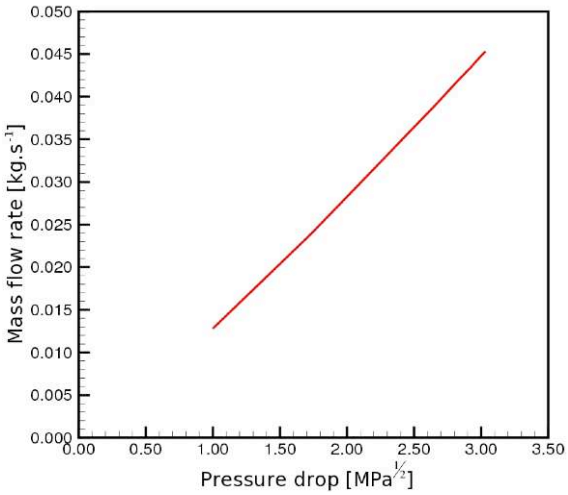

Figure 15: Mass flow rate versus the square root of the pressure drop

Figure 15 shows the mass flow rate evolution in regards of the square root of the pressure drop. An increase in the pressure difference between the inlet and exit of the orifice produces a corresponding increase in the flow rate.

Vapor phase seems to appear at a pressure drop of about 5.5 MPa. Then, it increases quickly when the back-pressure falls.

4. Conclusion

The first experiment presented this paper is still under progress. In the future, the quality of shadowgraphs should be improved by enhancing the index matching between test oil and PMMA. Velocity field measurements using FPIV are also planned and effect of orifice geometrical modifications (inlet radius, tapper, two-hole, etc.) will be carried out.

CFD calculations showed that it seems possible to obtain a cavitating flow with the 2D-nozzle geometric configuration presented in this paper. Future experiments will be carried out and the resulting data will be compared to these numerical results.

A CDF calculation (not presented in this paper) showed no roughness impact on the cavitating flow. However, some experimental studies [11, 14] shed light on a change in cavitation behavior du to roughness. The future experiments will help quantify this phenomenon by considering channel walls with different roughness (smooth, random roughness or textured).

This work is part of the French collaborative research program NADIA-bio supported by MOV'EO cluster.

5. References

[1] W. Bergwerk: "Flow pattern in diesel nozzle spray holes", Proceedings of the Institution of Mechanical Engineers, volume 173, 1959.

[2] N. Tamaki, M. Shimizu, K. Nishida and H. Hiroyasu: "Effects of cavitation and internal flow on atomization of a liquid", Atomization and Sprays, volume 8, issue 2, 1998.

[3] C. Soteriou, R. Andrews and M. Smith: "Direct injection diesel sprays and the e ect of cavitation and hydraulic flip on atomization", Society of Automotive Engineers, 1995.

[4] N. Tamaki, M. Shimizu and H. Hiroyasu: "Enhancement of the atomization of a liquid jet by cavitation in a nozzle hole", Atomization and Sprays, volume 11, issue 2, 2001.

[5] H. Hiroyasu: "Spray breakup mechanism from the hole-type nozzle and its applications", Atomization and Sprays, volume10, issues 3-5, 2000.

[6] D. D. Joseph: "Cavitation and state of stress in a flowing liquid", Journal of Fluid Mechanics, volume 366, 1998.

[7] S. Martynov, D. Mason, M. Heikal, S. Sazhin and M. Gorokhovski: "Modeling of cavitation flow in a nozzle and its effect on spray development", Proceedings of 13th International Heat Transfer Conference, Sydney, Australia, 2006.

[8] S. Dabiri, W. A. Sirignano and D. D. Joseph: "Cavitation in an orifice flow", Physic of Fluids, volume 19, issue 7, 2997.

[9] A. Sou, S. Hosokawa and A. Tomiyama: "Effects of Cavitation in a Nozzle on Liquid Jet Atomization", International Journal of Heat and Mass Transfer, volume 50, isuue 17-18, 2007.

[10] D. Schmidt, C. Rutland and M. L. Corradini: "A Numerical Study of Cavitating Flow Through Various Nozzle Shapes", Society of Automotive Engineers, 1997.

[11] E. Winklhofer, E. Kelz and A. Morozov: "Basic flow processes in high pressure fuel injection equipment", Proceedings of the 9th International Conference on Liquid Atomization and Spray Systems, Sorrento, Italy, 2003.

[12] F. Payri, V. Bermudez, R. Payri and F.J. Salvador: "The influence of cavitation on the internal flow and the spray characteristics in diesel injection nozzles", Fuel, volume 83, issues 4-5, 2004.

[13] H. K. Suh, S. H. Park and C. S. Lee: “Experimental investigation of nozzle cavitating flow characteristics for diesel and biodiesel fuels”, International Journal of Automotive Technology, volume 9, issue 2, 2008.

[14] C. Badock, R. Wirth, A. Fath and A. Leipertz: “Investigation of cavitation in real size diesel injection nozzles”, International Journal of Heat and Fluid Flow, volume 20, 1999.

[15] R. Saliba: “Investigation expérimentales sur les phénomènes de cavitation et d’atomisation dans les injecteurs diesel”, thesis, Ecole Centrale de Lyon, 2006.

[16] C. Arcoumanis, H. Flora, M. Gavaise and M. Badami: “Cavitation in real-size multi-hole diesel injector nozzles”, Society of Automotive Engineers, 2000.

[17] H. Chaves, M. Knapp, A. Kubitzek, F. Obermeier and T. Schneider: ”Experimental study of cavitation in the nozzle hole of diesel injectors using transparent nozzles”, Society of Automotive Engineers, 1990.

[18] G. H. Schnerr and J. Sauer: “Physical and Numerical Modeling of Unsteady Cavitation Dynamics”, Fourth International Conference on Multiphase Flow, New Orleans, USA, 2001.

[19] N. Dumont: “Modélisation de l’écoulement diphasique dans les injecteurs Diesel”, thesis, INP Toulouse, 2004.

[20] R. A. Bunnell, S. D. Heister, C. Yen and S. H. Collicott: “Cavitating injector flows: Validation of numerical models and simulations of pressure atomizers”, Atomization and Sprays, volume 9, issue 5, 1999.